Design of a heat treatment representative of the curing conditions of a massive concrete structure

Renaud Pierre Martin, François Toutlemonde

Design of a heat treatment representative of the curing conditions of a massive concrete structure

Renaud-Pierre MARTIN*
François TOUTLEMONDE
Université Paris-Est, Department of Structures and Structural Engineering, Paris, France

ABSTRACT

Delayed Ettringite Formation (DEF) is a concrete pathology that affects certain materials, depending on their composition, previously exposed at early age to a significant temperature rise (with a threshold of about 65 °C). During the casting of massive elements in particular, the combined effects of weak heat transfers and of the heat of hydration can lead to a significant temperature increase in the core of the structure inducing a major risk of DEF. In order to investigate the mechanical effects of this reaction to improve the management of the affected structures, studies are ongoing at the French Public Works Research (LCPC). This article describes the design of a heat treatment process that simulates the setting conditions in the core of a massive structure to induce DEF. The design concepts are presented in a first part, and describes in details the use of the QAB test to determine the heating phase. Then a numerical and experimental validation of this heat treatment is proposed in a second part.

Mise au point d'une cure thermique représentative de l'échauffement d'une pièce massive de béton

RÉSUMÉ

La réaction sulfatique interne (RSI) est une pathologie du béton qui affecte, suivant leur composition, certains matériaux ayant subi au jeune âge une élévation conséquente de leur température (seuil de l'ordre de 65 °C). Lors du coulage de pièces massives notamment, sous les effets combinés de transferts thermiques faibles et de l'exothermie de la réaction d'hydratation du ciment, la température à cœur peut augmenter de manière significative et induire des risques de RSI importants. Afin d'étudier les effets mécaniques de cette pathologie pour mieux gérer les ouvrages qui en sont atteints, des études sont en cours au LCPC. Cet article décrit la mise au point d'un procédé de cure thermique permettant de simuler les conditions de prise au cœur d'une structure massive afin d'induire des effets de RSI. Il présente dans un premier temps les concepts de dimensionnement considérés et notamment l'utilisation de l'essai QAB pour la détermination de la phase de chauffe. Ensuite, une validation numérique et expérimentale de la cure thermique est proposée.

***Corresponding author:**
Renaud-Pierre MARTIN
renaud-pierre.martin@lcpc.fr

INTRODUCTION

Delayed Ettringite Formation (DEF) is an endogenous reaction capable of damaging concrete structures: this pathology is characterized by material swelling, which in turn induces cracking as well as a deterioration in mechanical performance. In France, several tens of structures are presently

affected by this reaction **[1]**. Materials subjected to a significant temperature rise, beyond a threshold on the order of 65°C, at the early age are prone to this reaction **[2]**. As such, massive structures are found to be heavily exposed to this risk, with the combined effects of an exothermic cement hydration reaction and weak heat transfers leading to high and extended temperature rises at the core. These internal temperature variations cause ettringite dissolution-recrystallization mechanisms in the hardened material **[3, 4]**, thereby generating the disorders indicated above and providing the reason for serious issues encountered with physical integrity at the structural scale.

In order to develop a set of tools dedicated to reassessing impaired structures **[5]**, the French Public Works Laboratory (LCPC) is currently conducting an experimental study **[6]** intended to improve understanding of DEF mechanical effects at both the material scale (specimen testing) and structural scale (tests on beams) and thus further the work previously completed on the alkali-aggregate reaction **[7]**. To generate a "DEF potential", this experimental study proposes submitting materials after casting to a thermal treatment representative of the thermal and hydrological conditions under which setting takes place at the core of a massive concrete specimen. To apply a comparable thermal history for these various types of test samples, a specific approach has been adopted that incorporates the entire range of thermal mechanisms involved.

This article will present the methodology developed to achieve such a thermal treatment process. The next section will outline the methodological scope, with emphasis on the benefits of the QAB test in defining the heating phase. Afterwards, the components of a numerical validation exercise will be discussed, along with a thermal treatment model derived by implementing the CESAR-LCPC finite element computation code (TEXO module). The last section will describe an experimental validation of this treatment process.

THEORETICAL DEFINITION OF THE HEAT TREATMENT

Specifications

After casting, a heat treatment (also called thermal treatment) is to be applied to the test sample in an effort to recreate the maturation conditions that exist at the core of a massive element, including the temperature conditions capable of prevailing as a result of an exothermic cement hydration reaction. To facilitate a laboratory-based thermal treatment (via a considerable decrease in material cooling time compared with times experienced *in situ*), the actual temperature profile of the massive specimen has been simplified into a trapezoidal shape. The process then involves determining the various phases of: heating, constant temperature step, and the cooling necessary for completion of treatment.

The primary objective inherent in this thermal treatment is to apply a repeatable thermal history on the entire set of samples, for the purpose of producing materials with comparable "DEF potential": it has been possible to demonstrate **[8, 11]** that both the maximum temperature reached and the high temperature holding period exert influence on the potential DEF magnitude. The goal here consists of producing temperature deviations between the various specimens of less than ±1°C during the period of constant temperature. Moreover, application of a homogeneous temperature field to each specimen throughout this phase allows considering all parts of the structure to react identically, regardless of specimen size: temperature differences inside the same specimen must not exceed ±1°C, and the ultimate process be reproducible: any discrepancies in repeatability between two successive thermal treatments must remain below ±1°C during the constant temperature period. As a final constraint, the cooling phase must not cause cracking due to thermal shock.

Humidity

During production of a concrete element, cement hydration only uses a portion of the mixing water to form hydrates. Besides the porosity it generates after material drying, this excess water induces high relative humidity in the material at an early age. Experimental results **[9]** indicate that the relative humidity in small concrete prisms (measuring 76 × 76 × 280 mm^3) remains above 90% for more than 7 days, and this holds true even for specimens dried with a relative humidity equal to 50%.

In light of these findings, it was decided to conduct the thermal treatment in water, which not only provides for realistic application conditions given the humidity conditions prevailing at the core of a massive sample after casting, but also maintains specimens in a saturated state, which acts to promote DEF development. In addition, the creation of an actual thermal treatment device is facilitated when using water instead of humid air. Water also brings thermal inertia to the treatment system, which in turn allows for stricter temperature control with respect to external disturbances.

Heating phase

Given research program choices in terms of specimen size, the objective of this treatment consists of applying the same thermal history to both a set of beams (0.25 × 0.50 × 3.00 m^3) and cylindrical specimens (on the order of 0.1 m in diameter by a height of between 0.2 and 0.3 m), so as to generate an equivalent swelling potential from one specimen to another, as well as within the same specimen.

Due to the dimensions involved, temperature control at the beam core by means of applying a surface temperature boundary condition is difficult to implement, even more so at an early age when the predominant thermal mechanism is cement hydration. Furthermore, the thermal inertia of beams raises concerns over exceeding the temperature order during the heating phase - constant temperature step transition, i.e. the core of a beam only "feels" this change in heating mode belatedly relative to the beam surface. In contrast, the temperature of small-sized cylindrical specimens is easily controlled by the temperature setting in the treatment tank, thanks for the most part in this case to the abundance of thermal exchange phenomena (due to a greater exchange surface area / volume ratio for a given specimen, a low thermal inertia and a high heat transfer coefficient in water). These phenomena have been illustrated in **Figure 1**: for this particular example, temperature at the beam core displays deviations with respect to the treatment protocol that are much more pronounced than for a cylindrical specimen, which leads to substantial temperature variations between differently-sized specimens.

As a means of avoiding these scale effects, it was decided to simulate adiabatic conditions during the initial phase of temperature increase (**Fig. 3**): temperature history during the heating phase is tied to

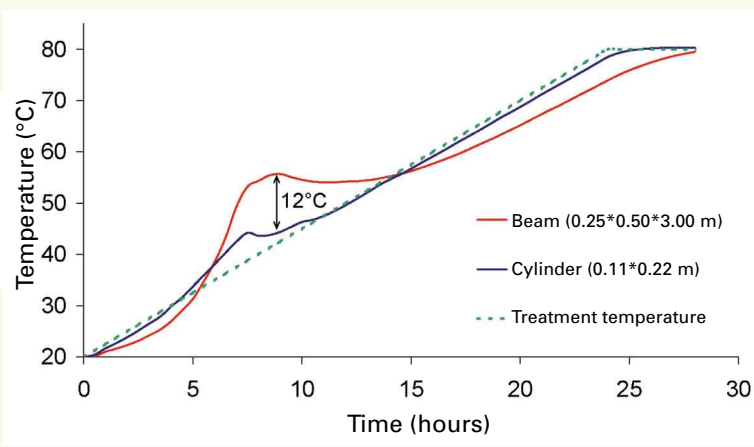

Figure 1
Temperature simulation at the core of concrete specimens subjected to heating (constant heating rate applied equal to 2.5°C/h)

temperature evolution, as determined by a QAB test, for the concrete mix under study. By limiting thermal transfers with the outside, this approach is able to ensure homogeneous temperature inside the specimen regardless of its size: this assurance offers control (from a theoretical standpoint) of treatment temperature as the temperature rises during cement hydration under adiabatic conditions. Moreover, this configuration enables recreating a temperature history resembling that of a massive element after casting, wherein the very weak exchange conditions lead to significant temperature increases at the time of cement hydration.

Constant temperature plateau

› Duration

At the end of the heating phase, specimens are exposed to a constant temperature step, which in addition to solubilizing the ettringite crystals previously formed during cement setting, allows adsorbing sulfates by the C-S-H structures, thus providing for a stockpile of reagents for subsequent DEF development **[3, 10]**. Expansion potential then increases with thermal treatment duration **[4, 8, 11]**. Measurements conducted on actual structures demonstrate that the temperature inside a massive element can remain above 70°C for eight full days **[12]**. Figure 2 simulates temperature changes at the core of a massive element 2 × 2 × 8 m^3 in size (these material characteristics are identical to those presented in the "Modeling set-up" section below, with an exchange coefficient on the side and bottom faces equal to 2.55 $W/m^2 \cdot °C$ - representative of a wooden formwork 20 mm thick - and an exchange coefficient on the exposed upper face equal to 10 $W/m^2 \cdot °C$, under conditions of a constant 20°C outdoor temperature): in this case, the temperature exceeds 70°C for more than 3 days.

In light of these findings, a 3-day threshold duration was established, as a compromise between the swelling potential provided by the thermal treatment and the organizational constraints associated with treatment duration.

Figure 2
Simulation of early-age temperature evolution at the core of a massive element (2 × 2 × 8 m^3)

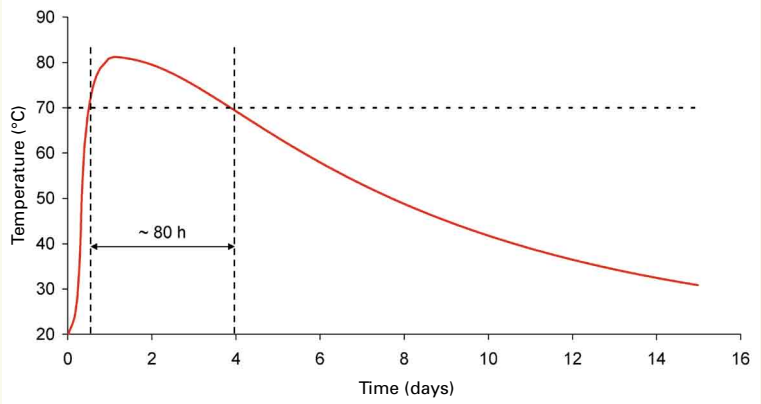

› Temperature

The heating phase simulates adiabatic conditions by adapting treatment temperature to the heat release, as determined while the QAB test is being run (*see* section entitled "Heating phase"). The temperature reached at the end of this phase can then be evaluated by calculating the rise in material temperature under adiabatic conditions. Waller proposed an approach to derive the value of this heat of hydration **[13]**; the present article will concentrate on the concrete mix design provided in Table 1. Equation (1) serves to calculate this temperature rise under adiabatic conditions **[13]**.

Table 1
Concrete mix design specifications (in kg/m^3)

Cement	Mixing water	0/2 siliceous sand	4/8 siliceous aggregate	8/12 siliceous aggregate	W/C
410	199	854	100	829	0.46

$$\Delta T(\infty) = \frac{Q(\infty)}{C_{th}} \quad (1)$$

According to this relation, $\Delta T(\infty)$ is the temperature rise experienced under adiabatic conditions at the end of cement hydration (expressed in K), $Q(\infty)$ the cement hydration heat at infinite time (in J/m³ of concrete), and C_{th} the average calorific capacity of concrete (in J/K/m³) evaluated on the basis of fresh concrete and the specific heat capacities of mix components at 20°C.

Cement hydration heat may be determined without any other information once the cement chemical composition is known **[13]**. **Table 2** lists the chemical composition of cement used in these study specimens. Waller **[13]** also suggested the specific hydration heat values given in **Table 3** for each cement phase. Cement heat of hydration can then be calculated by applying Equation **(2)**, where q_c is the specific heat of cement hydration (in J/g), q_i the heat of hydration of Phase i (in J/g), and ϕ_i the mass proportion of Phase i in the cement (in g/g). The numerical application of Equation (2) yields a specific heat of cement hydration equal to 384 J/g.

Table 2
Cement composition (according to Bogue's method)

C_3S	C_2S	C_3A	C_4AF	$CaSO_4$, $2H_2O$
41.5%	27.2%	5.0%	11.5%	7.4%

Table 3
Specific heat values of cement phase hydration, according to **[13]** *(in J/g)*

C_3S	C_2S	C_3A	C_4AF
510	260	1100	410

$$q_c = \sum_i (\phi_i \cdot q_i) \quad (2)$$

The cement heat of hydration at infinite time $Q(\infty)$ is to be calculated using Equation **(3),** in which $\alpha(\infty)$ is the final degree of hydration, c the cement concentration in the studied concrete mix (in g/m³) and q_c the specific heat of cement hydration (in J/g):

$$Q(\infty) = \alpha(\infty) \cdot c \cdot q_c \quad (3)$$

Based on a bibliographical review and from his own research results, Waller proposed Equation **(4)** below to derive the final degree of concrete hydration **[13]**, which for the concrete under study herein amounts to 0.78, for a *W/C* ratio of 0.46. With a cement concentration of 410 kg/m³, the heat release under adiabatic conditions at infinite time for the considered concrete is calculated to be: 123 000 kJ/m³.

$$\alpha(\infty) = 1 - e^{-3{,}3 \cdot \frac{E}{C}} \quad (4)$$

At this stage of the analysis, the specific heat of the concrete still needs to be calculated. For this purpose, Waller **[13]** proposed Equation **(5)**, where m_i is the quantity of component i in the mix (in g/m³) and c_i the specific heat of component *i* (in J/K/g). The specific heat of a cement can be assessed by means of a linear combination of the mass proportions of each cement phase and their corresponding specific heat, as indicated in **Table 4** **[13]**. The ensuing calculation produces a specific heat of the cement at 20°C equal to 0.72 J/K/g.

$$C_{th} = \sum_{i=components} m_i \cdot c_i^{th} \quad (5)$$

Table 4:
Specific heats of the various cement phases at 20°C **[13]** *(in J/K/g)*

C_3S	C_2S	C_3A	C_4AF	$CaSO_4$, $2H_2O$
0.745	0.740	0.768	0.815	1.074

In **[13]**, Waller provided a specific heat at 20°C of 0.73 J/K/g for siliceous aggregates and 4.19 J/K/g for water. To incorporate the drop in specific heat induced by the mobilization of water in a hydrate formation, AFNOR **[14]** suggested using a reduced specific heat of water set equal to 3.80 J/K/g, while Jolicœur **[15]** proposed decreasing specific heat as a function of bound water quantity, as per Equation **(6)**:

$$C_{th} = \sum_{i=components} m_i \cdot c_i^{th} - e_{bound} \cdot 2.0 \quad (6)$$

In this relation, the mass of bound water is evaluated by assuming it equal to 23% of the cement hydrate mass. Moreover, Waller introduced a fixed decrease in calorific capacity, in accordance with Equation **(7)**, making it possible to incorporate the change in concrete heat capacity under the hydration effect of the various cement phases. c is the cement content in the concrete composition (in kg/m^3) and α the degree of cement hydration.

$$C_{th} = \sum_{i=components} m_i \cdot c_i^{th} - 0.44 \cdot c \cdot \alpha(\infty) \quad (7)$$

Table 5 summarizes results of the specific heat calculation for concrete as a function of the adopted approach. The accuracy and precision of these volumetric specific heat values are not easy to measure: the cement hydration reaction proves, in reality, to be highly complex and leads to the formation of hydrates, each possessing its own specific heat. Furthermore, these specific heats actually vary with temperature. This approach however offers the double advantage of simplicity and ability to obtain estimations of the material calorific capacity without the need to run complex tests.

Lastly, depending on the approach adopted for evaluating the material specific heat, **Table 5** offers an evaluation of concrete temperature rise under adiabatic conditions, on the basis of Equation **(1)**. Since the specimens were produced at an average temperature of 20-25°C, the final temperature under adiabatic conditions will be in the range of 75-80°C. At this stage of the thermal treatment design, a threshold temperature of 80 ± 1°C has been selected.

Table 5
Estimation of both the specific heat of concrete (in kJ/K/m³) and associated temperature rise (°K) under adiabatic conditions

Calculation method	Without H_2O reduction (i.e. free water)	Fixed H_2O reduction (according to NF EN 196-9)	(Jolicœur, 1994)	(Waller, 2000)
Specific heat (kJ/K/m³)	2388	2314	2240	2247
Estimated temperature rise (°K)	51	53	55	55

Cooling

The thermal treatment for application to specimens concludes with a cooling phase. In order to both avoid specimen cracking due to thermal shock and ensure representativeness of the phenomena observed during fabrication of massive specimens, cooling speed has been set at –1°C/h. This phase also allows limiting total process duration in order to simplify laboratory procedures.

Treatment temperature profile

Based on the set of criteria defined above, the corresponding thermal treatment applied to test specimens has been depicted in **Figure 3**. The heating phase (with a duration of 24 hours and a maximum heating speed of 10°C/h) has been determined from results of a QAB test (**Fig. 3**) conducted for the specific concrete mix. Given the activation of diverse reactions initiated during the hydration of a cement sample, it is difficult to theoretically predict the associated heat release or its kinetics. It would be preferable therefore to proceed with an experimental determination of these parameters

Figure 3
Temperature evolution over the course of the heat treatment process

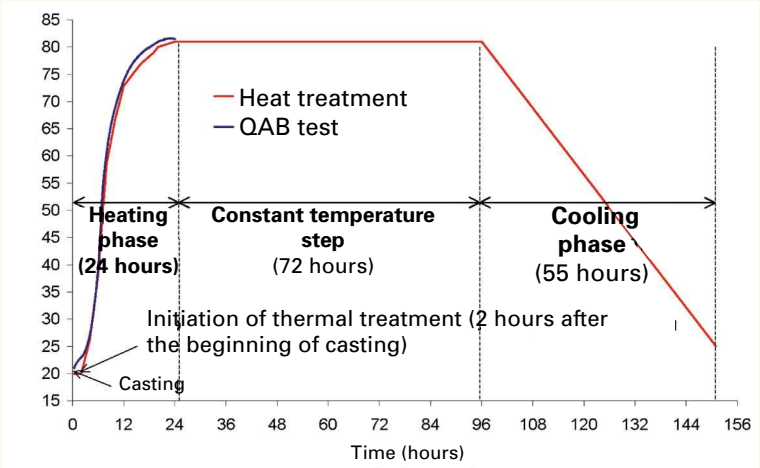

by means of a QAB test. The heating phase is initialized 2 hours after the beginning of specimen casting, since this time interval corresponds to the material placement phase in the laboratory. Next, a plateau is established at a temperature of 81°C, extending 72 hours (see previous section). Moreover, specimens are cooled at a speed of –1°C/h until reaching a temperature of 25°C. This process lasts a total of 151 hours, i.e. slightly longer than six days.

NUMERICAL SIMULATION OF THE THERMAL TREATMENT PROCESS

Modeling set-up

In order to assess the relevance of the treatment process developed in the preceding section, numerical models have been generated: through use of the TEXO module **[16–18]** included in the CESAR-LCPC finite element computation code **[19]**, the thermal treatment of a beam (measuring 0.25 × 0.50 × 3.00 m^3) and a cylinder (diameter = 0.11 m, height = 0.22 m) have both been simulated. The primary data input consists of the temperature rise under adiabatic conditions, obtained by running a QAB test. The other main characteristics and parameters of these calculations have been listed in **Table 6** and **Figure 4**. Both the thermal conductivity and specific heat of the material lie at orders of magnitude estimated to be representative of an ordinary concrete. The heat transfer coefficient was

Figure 4
Meshes and post-processing points: a) beam; b) Specimens 11-22

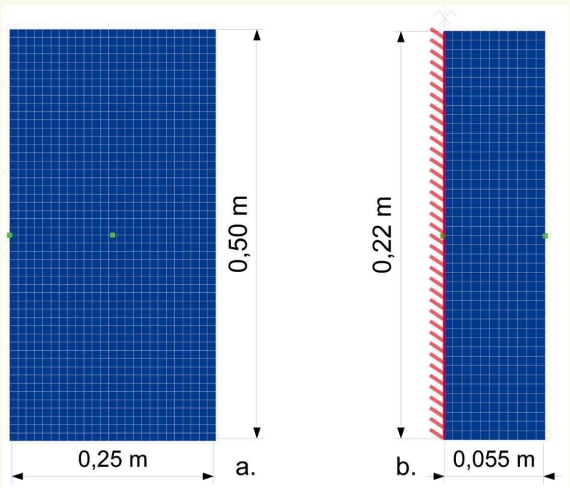

Table 6
TEXO module characteristics

Beam model		2D
Specimen model		2D, axisymmetric
Formwork/water heat exchange coefficient		100 W/(m²°C)
Thermal conductivity	K_x	1.67 W/(m°C)
	K_y	1.67 W/(m°C)
	K_{xy}	0 (isotropic conductivity)
Specific heat of hardened concrete, C_{th}		2400 kJ/(m³ K)

set at a value of 100 W/(m² · °C), which is the order of magnitude of the exchange coefficient in water **[20]**. Moreover, a sensitivity analysis of results to this parameter has indicated that increasing the heat transfer coefficient by a factor of 10 only induces a slight deviation in the temperature field evaluation for specimens covered in our calculation protocol.

Theoretical thermal response of a beam

Figure 5 shows the evolution in temperature at both the center and edge of the common cross-section of a beam during heat treatment. These results highlight one of the benefits of a pseudo servo-control of heating speed as the material heats under adiabatic conditions: a relatively homogeneous temperature field is obtained in the specimen (**Figs 5** and **6**) during heating, despite high heating speeds, in order to reach the thermal treatment plateau. At the heating phase-temperature plateau transition, the targeted value is only exceeded by a very slight margin at the beam core: the proposed approach thus enables considerably limiting the thermal inertia effects of a specimen of this type.

Figure 5b provides the evolution in temperature difference between the beam center and edge (**Fig. 4a**) over the course of the treatment process; this difference remains less than 4°C during the heating phase and narrows to around 3°C during cooling. Over the entire temperature plateau period (i.e. between t = 24 and 96 hours), this difference lies near zero. From a theoretical standpoint, the thermal treatment defined herein is able to meet the temperature field homogeneity criterion established in the protocol specifications.

Figure 5
a) Theoretical thermal response of a beam to the treatment process; and b) deviation in the corresponding temperature between the center and edge of a section

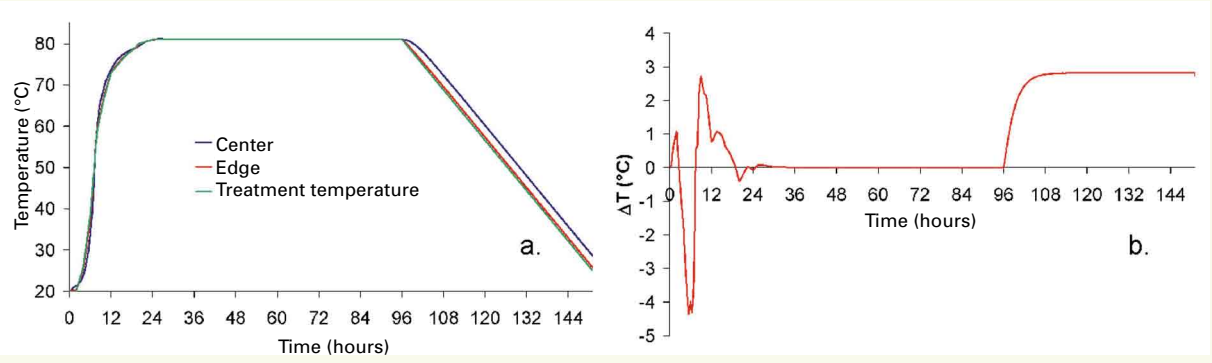

Dimensional influence: Theoretical evaluation

Figure 7 reflects the deviations in theoretical temperature between a beam core and the core of a smaller specimen (**Fig. 4**). These results underscore the small discrepancy existing between these two types of samples during the threshold phase (from t = 24 to t = 96 hours), in compliance with the designated protocol specifications. In the heating phase, this deviation climbs to as high as 5°C during the most intensive heating (10°C/h). This effect is primarily correlated with the differences

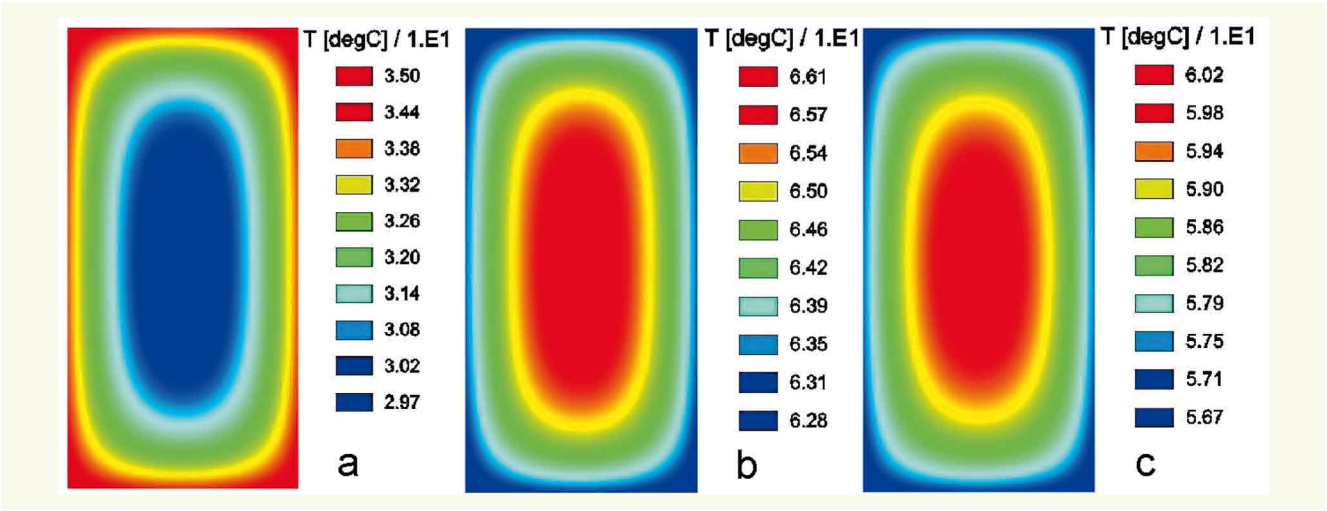

Figure 6
Temperature fields inside a beam at: a) t = 5.5 hours; b) t = 9 hours; c) t = 120 hours

in thermal inertia between the two elements: it winds up being easier to control the temperature at the core of a small-sized specimen, by imposing a boundary condition, rather than the temperature of a beam. The strong similarity of **Figures 5b** and **7** is worth noting: temperature at the core of a specimen remains very close to treatment temperature throughout the process. This interpretation would also be applicable to the deviations observed during cooling.

Figure 7
Temperature deviation between the beam core and a specimen

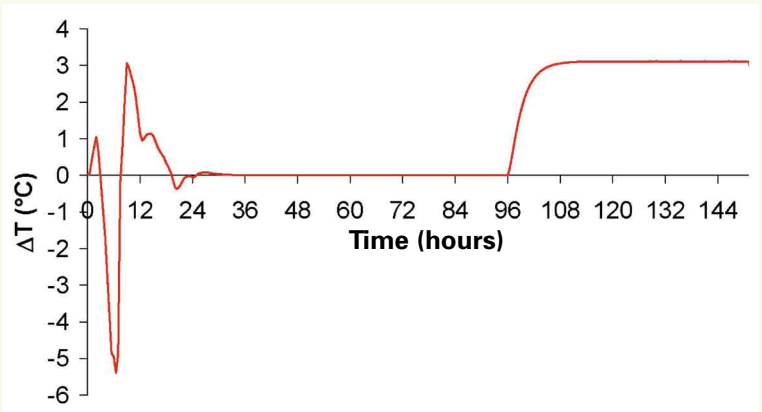

Sensitivity study: Influence of a change in cement

Figure 8a compares the temperature evolution inside a QAB calorimeter and under adiabatic conditions (i.e. once thermal losses have been corrected and thermoactivation included) of both a concrete specimen chosen for these thermal treatment specifications (Concrete 1: *see* Section entitled "Heating phase") and a less exothermic concrete (Concrete 2). The chemical composition of the corresponding cement is listed in **Table 7**. In calculating the equivalent age, an average ratio of E_a/R 5000 K has been assumed as part of this initial approach. Given the lack of complementary data, this value was considered as representative of the types of concretes under study. Undertaking QAB tests at different temperatures would serve to improve the accuracy of this estimation **[21]**.

Table 7
Composition of the cement used in Concrete 2 (according to Bogue's method)

C_3S	C_2S	C_3A	C_4AF	$CaSO_4$, $2H_2O$
43.2%	2.2%	2.4%	11.6%	5.6%

Figure 8b displays the thermal responses of the beams built using these two concretes. In the case of Concrete 2, a QAB type approach with a "sigmoid" pattern heating phase still proves to be somewhat efficient, as the observed temperature deviations with respect to the temperature order

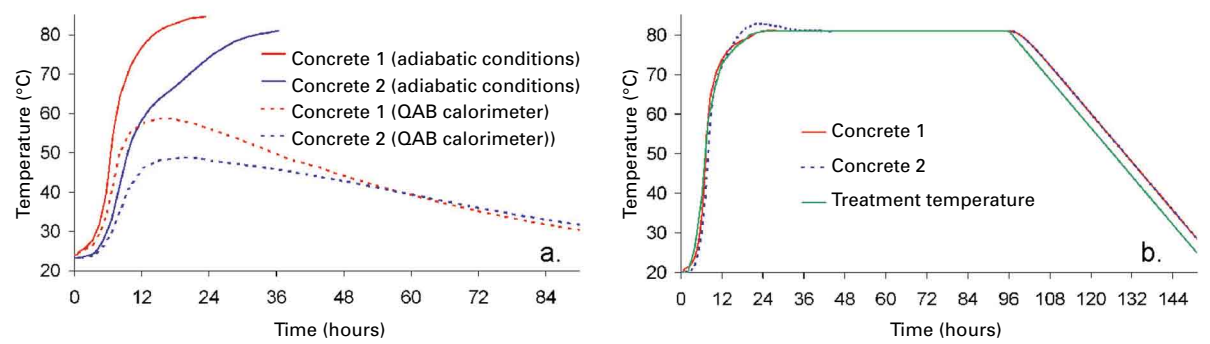

Figure 8
a) Heat release of concretes; and b) thermal response (temperature at the specimen core) of the corresponding beams

are comparatively less than those generated under constant heating speed (*see* **Fig. 1**). On the other hand, the recommended guideline at the specimen core is greatly surpassed between t = 14 and t = 30 hours. This example reveals therefore the benefit of identifying a calibrated heating phase in the studied concrete by performing a QAB test, for the purpose of minimizing temperature deviations inside the treated specimen.

EXPERIMENTAL VALIDATION OF THE THERMAL TREATMENT PROCESS

Experimental set-up

Practically speaking, as part of the research conducted at LCPC beginning in 2006 on the mechanical effects of DEF, thermal treatments have been conducted using a device specifically designed for this study **[6]**: a tank filled with water whose temperature is regulated by means of a 24-kW immersion heater guided by a programmable device (**Fig. 9a**), into which specimens are immersed after casting. Temperature homogeneity in this tank is maintained by stirring the water via pump action. This set-up does not include any cooling system: the temperature is lowered by natural cooling at first (through the temperature differential between the tank and the outside), then by injecting cold water into the water circuit.

Performance tests made it possible to guarantee that during a constant temperature step, temperature may be regulated to an accuracy of ±0.5°C with respect to the temperature order. This process is repeatable, also to an accuracy of ±0.5°C, in acknowledging the level of uncertainty on temperature measurements. Temperature homogeneity in the tank has been verified, yielding maximum temperature differences in the tank of 1°C during heating phases.

Figure 9
a) Thermal treatment device; and b) experimental demonstration of the treatment

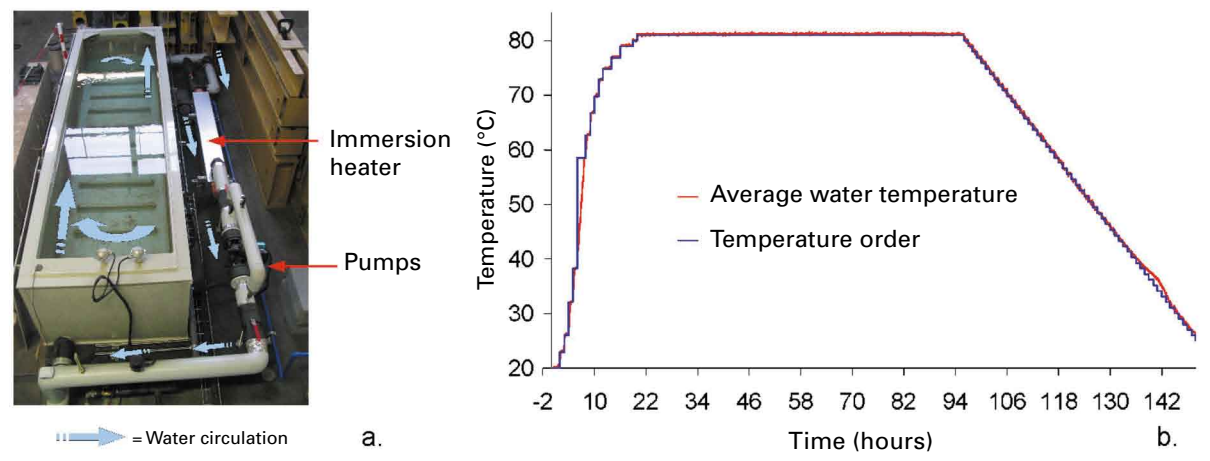

Figure 9b illustrates an experimental approximation to this thermal treatment via such a device. A deviation can be observed at the end of cooling between temperature of water and the temperature order (maximum deviation found to be on the order of 2°C): at this stage of the process, reducing the temperature deviation between the tank and the outside would hinder the natural cooling capacities of the system. According to this scenario, cooling is forced by increasing the flow rate of cold water injection.

Experimentally-derived thermal response of a beam

With the aim of experimentally evaluating the behavior of a beam during this thermal treatment, a specimen has been instrumented along a common cross-section (located 0.6 m from the longitudinal extremity) using temperature sensors at points denoted M1, M2, M3, M4 and M5, positioned respectively at depths of 0.04 m, 0.08 m, 0.17 m, 0.27 m and 0.37 m relative to the upper beam

Figure 10
Experimental thermal response of a beam: Heating phase

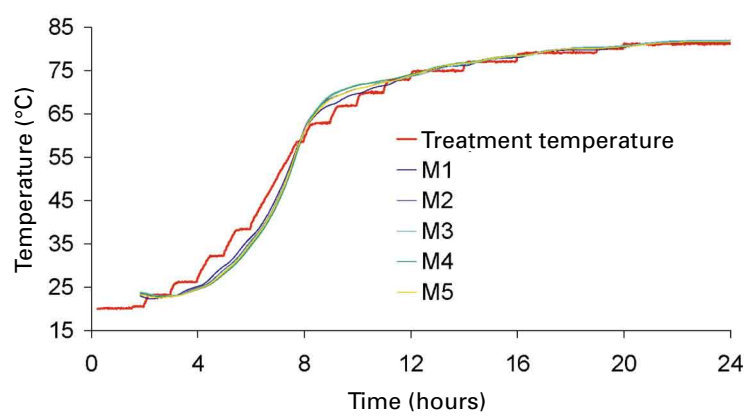

Figure 11
Experimental thermal response of a beam: Temperature plateau

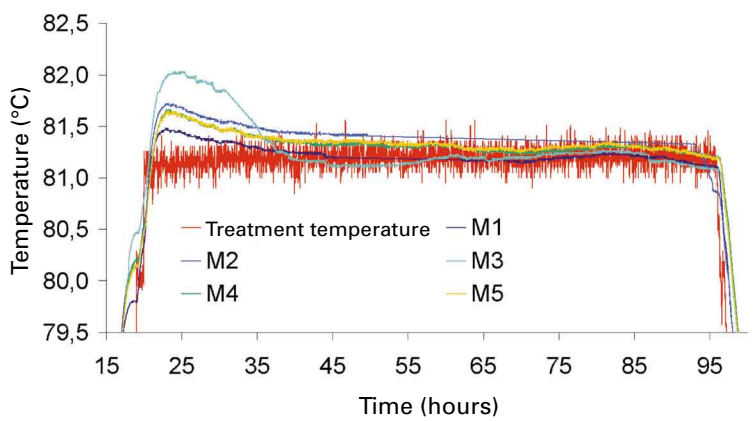

Figure 12
Experimental thermal response of a beam: Cooling phase

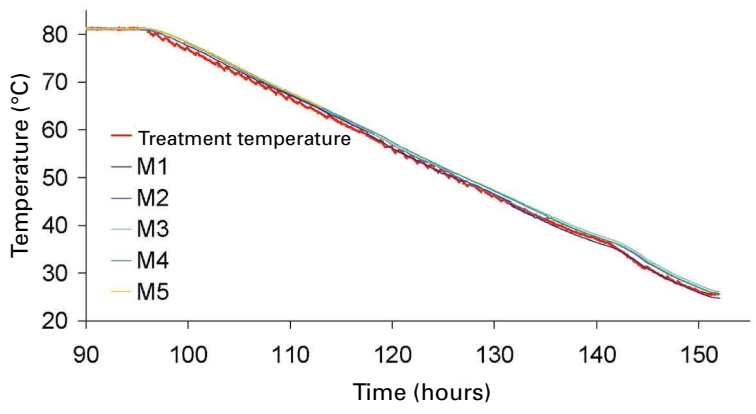

face. **Figures 10-12** show the temperature evolution at these specific spots during the heating phase, constant temperature step and cooling phase, respectively.

It can be noticed that experimental behaviour, on the whole, agrees with the modeling output presented in the previous section. During the heating phase, temperature deviations at the various instrumented points remain below ±2°C despite the heating speeds. This finding experimentally confirms the benefit of calibrating the heating phase on results from the QAB test, corresponding to the concrete under study, thereby ensuring the most homogeneous temperature field possible in a specimen with high thermal inertia. These temperature differences do not exceed ±0.5°C during the constant temperature step, hence in compliance with the criterion established in process specifications. During the heating phase - plateau transition however, the treatment guideline is slightly surpassed within the beam, to a level of approx. 1°C over about 10 hours. Moreover, during the cooling phase, these deviations remain less than 1°C until reaching a temperature of roughly 45°C, at which point it becomes more difficult to maintain constant cooling speed (*see* section above). Beyond this temperature, all differences lie below 2°C. These results have made it possible to validate the thermal treatment process with respect to the temperature field homogeneity criterion.

Figure 13 compares the evolution in temperature at point M4 during the heating phase, according to whether it has been obtained experimentally or numerically. TEXO module predictions turn out to be in agreement with the practical conception of thermal treatment. Nonetheless, it is remarked that beginning at $t = 8$ hours, the model shows a tendency to underestimate temperature at the beam core (with a maximum deviation of around 3°C). This observation may be explained by a difference in how fast the cement hydration reaction is progressing at this specific instant, with such a difference stemming from the discrepancy in experimental and theoretical thermal states at the time of casting. While the model takes into account a material placed at a temperature of 20°C, the experimental protocol demonstrates that this hypothesis is difficult to accurately satisfy (*see* **Fig. 10**, $t = 2$ hours), due to the room temperature at the time of specimen production or to the mixing effect.

Figure 13
Heating phase temperature at point M4 (at a depth of 0.27 m)

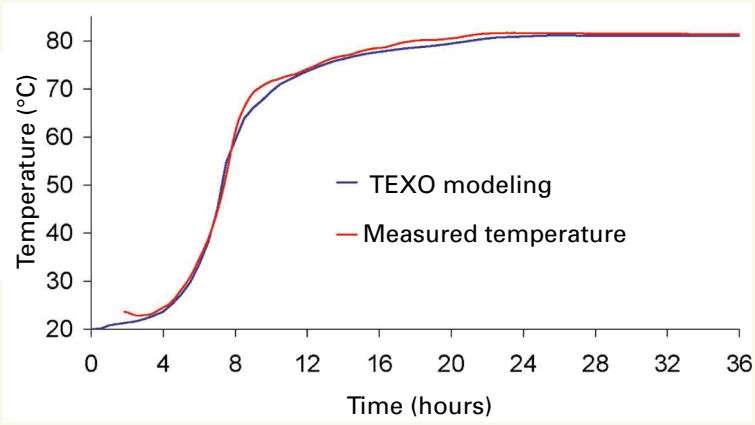

Figure 14 offers the evolution in temperature differential between points M4 and M1 throughout the treatment process. These results highlight the good correlation between predicted thermal behavior and behavior observed during the experimental campaign. It has been found this time however that the model overestimates the deviation during cooling; over this treatment phase, hydration reactions only constitute a small fraction of the thermal phenomena governing specimen behavior, with exchange-induced losses becoming predominant. It is likely for the observed differences at this point to be correlated not only with an overestimation of the beam specific heat (a complicated correlation to evaluate as a result of its dependence on both temperature and degree of hydration reaction progress), but also with an underestimation of the formwork/water exchange coefficient. These deviations however remain limited.

The results presented in this section showcase the relevance of a numerical modeling set-up using the TEXO module for refining the treatment procedure prior to a full experimental campaign.

Figure 14
Temperature deviations between points M4 (0.27 m deep) and M1 (0.04 m)

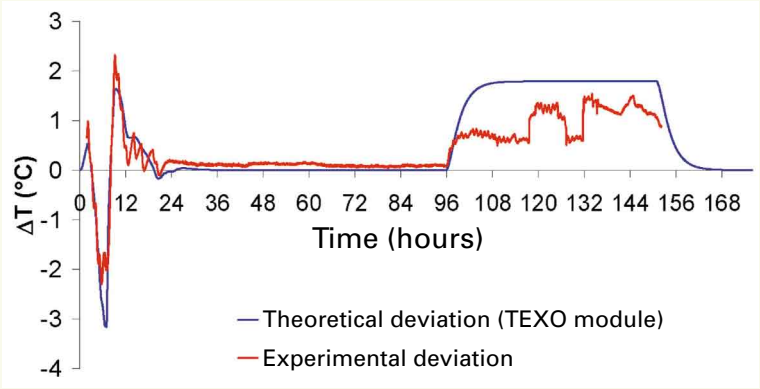

Controlling for scale effects: Experimental evaluation

Figure 15 presents the temperature deviation existing between the core of a cylindrical specimen (diameter = 0.11 m; height = 0.22 m) and a beam core (according to both numerical and experimental approaches). During the heating phase, a comparable thermal behavior can be observed regardless of the approach adopted. Nonetheless, the differences in initial thermal state lead to maximum deviations on the order of 3°C between model output and experimental findings. Throughout the temperature constant period, temperature differences between specimens remain below 1°C, thus satisfying the established target (*see* section entitled "Treatment specifications"). Moreover, during cooling, an overestimation of this deviation is once again apparent for the same reasons cited above (i.e. evaluation of specific heats and heat transfer conditions). In the end, the experimental depiction of this treatment process on a beam and a smaller specimen has served to validate the process relative to its objective, which consists of applying a similar thermal history to differently-sized specimens.

Figure 15
Temperature deviation between the core of a beam (Point M4) and a smaller specimen core

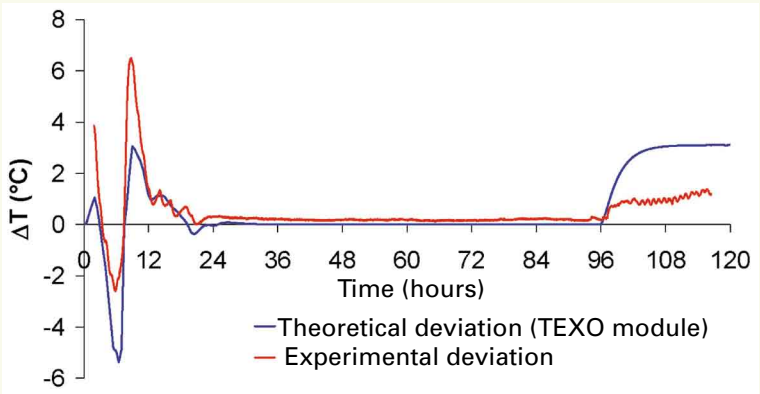

Repeatability considerations

In an effort to assess the repeatability of this thermal treatment process, several beams of identical composition and dimensions underwent thermal monitoring. **Figure 16a** gives the evolution in temperature within each specimen at a depth of 0.27 m from the upper surface (Point M4). The main differences between beams are noticeable: at the beginning of the heating phase and under the effect of variable initial thermal states (which may be ascribed to the variation in room temperatures at the time of the various casting steps, i.e. between 20°C and 25°C); and at the end of cooling, when it becomes more difficult to control treatment tank temperature due to the effect of the surrounding air temperature. **Figure 16b** proposes a graph to describe temperature deviations between specimens over time. Deviations are highest during roughly the first 10 hours of treatment: the influence

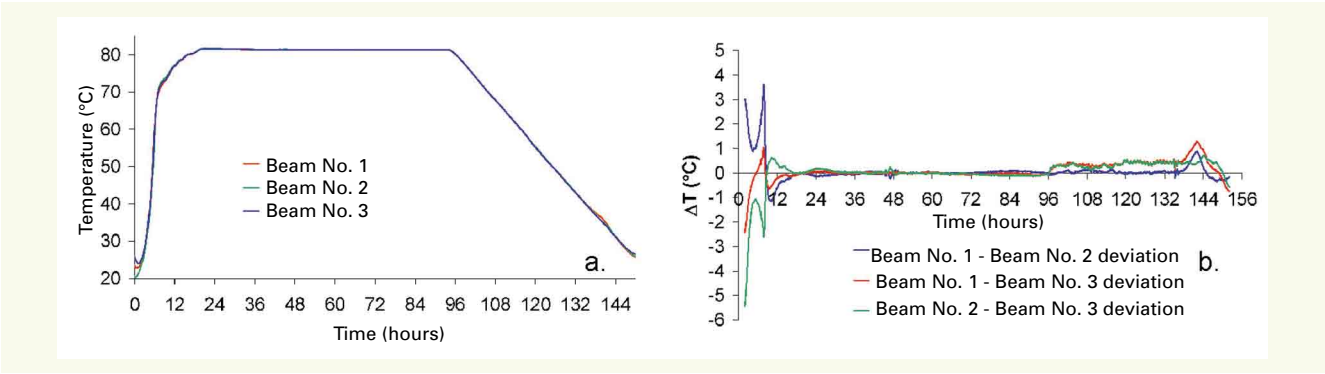

Figure 16

a) Thermal monitoring of three identical beams during the treatment process (Point M4); b) corresponding temperature deviations

of material placement temperature is dominant over this stretch of time. Once the intense heating phase has been completed, these deviations decrease substantially. During the temperature threshold, differences remain below the ±1°C limit stipulated in the process specifications.

CONCLUSION

This article has presented the methodology implemented in order to design a heat treatment process that generates DEF swelling. Applied to the material after casting, this process is intended to simulate concrete setting conditions at the core of a massive element. One of the main objectives assigned to this thermal process has consisted of applying a similar thermal history to specimens of all sizes.

One critical aspect of this thermal treatment lies in calibrating material heating speeds during the early age to temperature increases under adiabatic conditions, as measured by means of a QAB test. It therefore becomes possible to simulate the adiabatic conditions for concrete elements, which enables minimizing the thermal effects tied to their inertia as well as ensuring a better homogeneity of their temperature field.

A numerical study of the process has also been performed. Based on a finite element modeling set-up using the TEXO module of the CESAR-LCPC computation code, this study has provided an initial approach to estimating the relevance of a temperature profile during treatment, with respect to both the thermal field homogeneity criterion and scale effects (via a comparison of temperatures in beams and smaller specimens).

Lastly, an experimental validation of the thermal treatment was carried out. Once the performance of the customized device had been verified, we highlighted the benefits of this thermal treatment relative to the application of a homogeneous and repeatable temperature field for all types of specimens.

Such a treatment process may be introduced regardless of the specific concrete mix design; it is merely necessary to know the level of heating experienced by the material during setting under adiabatic conditions, which can be easily determined from a QAB test.

ACKNOWLEDGMENTS

The authors would like to thank LCPC's Structural Experimentation and Modeling unit and in particular F.-X. Barin, C. Bazin, J. Billo, M. Estivin, L. Lauvin and J.-C. Renaud for their valuable assistance throughout the experimental phase of thermal treatment validation, as well as D. Siegert (with the Department of Measurement, Monitoring and Scientific Computations), whose participation proved determinant during development of this treatment process. The authors are also grateful for the support provided by EDF (E. Bourdarot, A. Jeanpierre) towards the research program devoted to the mechanical effects of DEF.

REFERENCES

1 **Kretz T.**, **Godart B.** & **Divet L.** (sous la direction de), *Recommandations pour la prévention des désordres dus à la réaction sulfatique interne*, LCPC, Guide technique, **2007**, 59 pages.

2 **Divet L.**, Les réactions sulfatiques internes au béton : contribution à l'étude des mécanismes de la formation différée de l'ettringite, LCPC, ERLPC, OA 40, **2001**, 227 pages.

3 **Barbarulo R.**, **Peycelon H.**, **Leclercq S.**, Chemical equilibria between C-S-H and ettringite, at 20 and 85 °C, *Cement and Concrete Research*, vol. **37**, **2007**, pp. 1176-1181.

4 **Taylor H. F. W.**, **Famy C.**, **Scrivener K. L.**, Delayed ettringite formation, *Cement and Concrete Research*, vol. **31**, n° 5, **2001**, pp. 683-693.

5 **Mahut B.** & **Fasseu P.** (sous la direction de), *Aide à la gestion des ouvrages atteints de réactions de gonflement interne*, LCPC, Guide technique, **2003**, 66 pages.

6 **Martin R.-P.**, **Siegert D.**, **Toutlemonde F.**, Experimental analysis of concrete structures affected by DEF, *3rd International Symposium GEOPROC'2008*, Lille (France), 2-4 juin, **2008**, pp. 589-596.

7 **Multon S.**, Évaluation expérimentale et théorique des effets mécaniques de l'alcali-réaction sur des structures modèles, LCPC, ERLPC, OA 46, **2004**, 423 pages.

8 **Brunetaud X.**, Étude de l'influence de différents paramètres et de leurs interactions sur la cinétique et l'amplitude de la RSI au béton, Thèse de l'École Centrale de Paris, Paris, **2006**, 253 pages.

9 **Grasley Z. C.**, **Lange D. A.**, **D'Ambrosia M. D.**, **Villalobos-Chapa S.**, Relative Humidity in concrete, *ACI Committee*, **236**, **2006**, pp. 51-57.

10 **Pavoine A.**, Évaluation du potentiel de réactivité des bétons vis-à-vis de la formation différée de l'ettringite, Thèse de l'Université Pierre et Marie Curie, Paris, **2003**, 229 pages.

11 **Baghdadi N.**, **Seignol J.-F.**, **Martin R.-P.**, **Renaud J.-C.**, **Toutlemonde F.**, Effect of early age thermal history on the expansion due to delayed ettringite formation: experimental study and model calibration, *Advances in Geomaterials and Structures Conference 2008 (AGS 2008)*, Hammamet (Tunisie), 5-7 mai, **2008**, pp. 661-666.

12 **Divet L.**, Comment se prémunir des réactions sulfatiques dans les bétons ?, *Bulletin des Laboratoires des Ponts et Chaussées*, vol. **240**, **2002**, pp. 87-94.

13 **Waller V.**, Relations entre compositions des bétons, exothermie en cours de prise et résistance en compression, *LCPC*, ERLPC, OA **35**, **2000**, 316 pages.

14 **AFNOR**, NF EN 196-9 Méthodes d'essais des ciments – Partie 9 : Chaleur d'hydratation – Méthode semi-adiabatique, AFNOR, **2004**, 20 pages.

15 **Jolicœur C.**, **Bilodeau J.**, **Simard M.A.**, Étude calorimétrique de l'hydratation du ciment – Détermination de l'énergie d'activation, Rapport d'étape, rapport interne LCPC, **1994**.

16 **Torrenti J.-M.**, *Comportement mécanique du béton – Bilan de six années de recherche*, LCPC, ERLPC, OA **23**, **1996**, 109 p.

17 **Ulm F.-J.**, Couplages thermomécaniques dans les bétons – Un premier bilan, LCPC, ERLPC, OA **13**, **1999**, 105 p.

18 **D'Aloia L.** & **Chanvillard G.**, Determining the "apparent" activation energy of concrete Ea – numerical simulations of the heat of hydration of cement, *Cement and Concrete Research*, vol. **32**, **2002**, pp. 1277-1289.

19 **Humbert P.**, **Dubouchet A.**, **Fezans G.**, **Remaud D.**, CESAR-LCPC, un progiciel de calcul dédié au génie civil, *Bulletin des Laboratoires des Ponts et Chaussées*, vol. **256-257**, **2005**, pp. 7-37.

20 **Lienhard J.H. IV** & **Lienhard J.H. V**, *A heat transfer textbook*, Phlogiston Press, Cambridge, Massachussetts, 3e édition, **2008**, 749 p.

21 Sous la direction de **Buyle-Bodin F.** & **Cussigh F.**, *Résistance du béton dans l'ouvrage – La maturométrie*, LCPC, Guide technique, **2003**, 66 p.